Masters thesis

The Hopf Hopf Bifurcation

Hengki Tasman
Supervisor: H.W. Broer

Rijksuniversiteit Groningen
Department of Mathematics
Postbus 800
9700 AV Groningen

December 2001

The Hopf Hopf Bifurcation

Hengki Tasman

December 19, 2001

Abstract

This paper studies 4-dimensional dynamical systems whose linear parts are doubly degenerate and no low-order resonances occur. It also explore some persistent properties of the systems, including the interesting 3-quasi periodicity.

Contents

1 Introduction

1.1 Setting of problem

Consider a dynamical system:

$$\dot{\mathbf{x}} = X(\mathbf{x}), \tag{1}$$

where $\mathbf{x} \in \mathbb{R}^4$, $X \in C^\infty(\mathbb{R}^4, \mathbb{R}^4)$. We assume that $\mathbf{x} = 0$ is the equilibrium of this system and also that the linear part of this system at its equilibrium (D_0X) is doubly degenerate, that is, it has two distinct pure imaginary pairs of eigenvalues. Without restriction of generality, we let the linear part take the form:

$$\begin{bmatrix} \dot{x} \\ \dot{y} \\ \dot{z} \\ \dot{v} \end{bmatrix} = \begin{bmatrix} 0 & -\omega_1 & 0 & 0 \\ \omega_1 & 0 & 0 & 0 \\ 0 & 0 & 0 & -\omega_2 \\ 0 & 0 & \omega_2 & 0 \end{bmatrix} \begin{bmatrix} x \\ y \\ z \\ v \end{bmatrix}. \tag{2}$$

Furthermore, let us assume that no low-order resonances occur, specifically that $m\omega_1 + n\omega_2 \neq 0$, for all integers m and n with $|m| + |n| \leqslant 4$.

For this system there is no finite classification modulo topological equivalence [3, 4, 5]. In this paper we will give a generic description of it.

1.2 Outline

In Section 2 we bring the system into a normal form by applying proper choices of coordinate transformations. Then we introduce unfolding parameters. After this, we make the normal form as simple as possible, by rescaling the variables and reversing time.

Section 3 explores the unperturbed system of (1). We first consider the two-dimensional reduced unperturbed system at its central codimension two singularity, and then its unfolding. After that, we reconstruct the results into its four dimensional setting.

In the last section we restore the higher order terms and list which properties are persistent and which are not.

2 Normal form

The idea of normalization is to expand the vector field X in Taylor series at its equilibrium, and simplify the series by proper choices of coordinate transformations. In this section, we quote a normal form theorem which helps us to obtain a simple form of system (1) near its equilibrium.

Consider a vector field $\dot{\mathbf{x}} = X(\mathbf{x})$, with $X(\mathbf{x}) = A\mathbf{x} + f(\mathbf{x})$, $\mathbf{x} \in \mathbb{R}^n$, where A is linear, $f(0) = 0$, $D_0 f = 0$. Define the adjoint action $\mathrm{ad}A$ by the Lie-bracket

$$\mathrm{ad}A : Y \mapsto [A\mathbf{x}, Y],$$

for a vector field $Y \in C^\infty(\mathbb{R}^n, \mathbb{R}^n)$. Let $H^m(\mathbb{R}^n)$ be a space of polynomial vector fields, homogeneous of degree m. The action $\mathrm{ad}A$ induces a linear map $H^m(\mathbb{R}^n) \to H^m(\mathbb{R}^n)$. Let $B^m = \mathrm{im}\ \mathrm{ad}_m A$, and G^m is a complement of B^m in $H^m(\mathbb{R}^n)$, i.e., $G^m \bigoplus B^m = H^m(\mathbb{R}^n)$.

Theorem 1 [7, 11] *Let X be a C^∞ vector field, defined in the neighbourhood of $0 \in \mathbb{R}^n$, with $X(0) = 0$ and $D_0 X = A$. Also let $N \in \mathbb{N}$ be given. If no resonances occur up to order $N+1$, i.e. $k\omega_1 + l\omega_2 \neq 0$, for all integers k and l with $1 \leqslant |k| + |l| \leqslant N+1$, then there exists, near $0 \in \mathbb{R}^n$, an analytic change of coordinates $\Phi : \mathbb{R}^n \to \mathbb{R}^n$, with $\Phi(0) = 0$, such that*

$$\Phi_* X(y) = Ay + g_2(y) + \cdots + g_N(y) + O(|y|^{N+1}),$$

with $g_m \in G^m$, for all $m = 2, 3, ..., N$.

Applying Theorem 1, the third order normal form of system (1) is

$$\begin{aligned}
\dot{x} &= -\omega_1 y + a_{11}x(x^2+y^2) + a_{12}x(z^2+v^2) + a_{13}y(x^2+y^2) \\
&\quad -a_{14}y(z^2+v^2) + O(|x,y,z,v|^5) \\
\dot{y} &= \omega_1 x + a_{11}y(x^2+y^2) + a_{12}y(z^2+v^2) - a_{13}x(x^2+y^2) \\
&\quad +a_{14}x(z^2+v^2) + O(|x,y,z,v|^5) \\
\dot{z} &= -\omega_2 v + a_{21}z(x^2+y^2) + a_{22}z(z^2+v^2) - a_{23}v(x^2+y^2) \\
&\quad -a_{24}v(z^2+v^2) + O(|x,y,z,v|^5) \\
\dot{v} &= \omega_2 z + a_{21}v(x^2+y^2) + a_{22}v(z^2+v^2) + a_{23}z(x^2+y^2) \\
&\quad +a_{24}z(z^2+v^2) + O(|x,y,z,v|^5),
\end{aligned} \tag{3}$$

where $a_{11}, a_{12}, a_{13}, a_{14}, a_{21}, a_{22}, a_{23}, a_{24}$ are coefficients.

A versal unfolding (or versal deformation) of this system is given by

$$\begin{aligned}
\dot{x} &= \mu_1 x - \omega_1 y + a_{11}x(x^2+y^2) + a_{12}x(z^2+v^2) + a_{13}y(x^2+y^2) \\
&\quad -a_{14}y(z^2+v^2) + O(|x,y,z,v|^5) \\
\dot{y} &= \mu_1 y + \omega_1 x + a_{11}y(x^2+y^2) + a_{12}y(z^2+v^2) - a_{13}x(x^2+y^2) \\
&\quad +a_{14}x(z^2+v^2) + O(|x,y,z,v|^5) \\
\dot{z} &= \mu_2 z - \omega_2 v + a_{21}z(x^2+y^2) + a_{22}z(z^2+v^2) - a_{23}v(x^2+y^2) \\
&\quad -a_{24}v(z^2+v^2) + O(|x,y,z,v|^5) \\
\dot{v} &= \mu_2 v + \omega_2 z + a_{21}v(x^2+y^2) + a_{22}v(z^2+v^2) + a_{23}z(x^2+y^2) \\
&\quad +a_{24}z(z^2+v^2) + O(|x,y,z,v|^5),
\end{aligned} \tag{4}$$

where μ_1 and μ_2 are parameters. For a detailed description of versal unfoldings, we refer to Arnold [1] and Chow, Li & Wang [10].

For convenience, we write this latter system in the toroidal coordinates ($x = r_1\cos(\theta_1)$, $y = r_1\sin(\theta_1)$, $z = r_2\cos(\theta_2)$, and $v = r_2\sin(\theta_2)$ [1]). To reduce the number of coefficients we perform a rescaling, given by, $\bar{r}_1 = r_1\sqrt{|a_{11}|}$ and $\bar{r}_2 = r_2\sqrt{|a_{22}|}$. By dropping the bar and, if necessary, reversing the time, we obtain:

$$\begin{aligned}
\dot{r}_1 &= r_1(\mu_1 + r_1^2 + br_2^2) + O(|r_1, r_2|^5) \\
\dot{r}_2 &= r_2(\mu_2 + cr_1^2 + dr_2^2) + O(|r_1, r_2|^5) \\
\dot{\theta}_1 &= \omega_1 + O(|r_1, r_2|^2) \\
\dot{\theta}_2 &= \omega_2 + O(|r_1, r_2|^2),
\end{aligned} \tag{5}$$

where $b = a_{12}/|a_{22}|$, $c = a_{21}/|a_{11}|$ and $d = a_{22}/|a_{22}| = \pm 1$.

3 The unperturbed system

Dropping the higher order terms of (5), we get an (unperturbed) system of (1). To understand its dynamical properties, first we drop the azimuthal components ($\dot{\theta}_1$ and $\dot{\theta}_2$), since they are decoupled from the radial components ($\dot{r}_1$ and $\dot{r}_2$). Next we analyze the properties of the reduced system, afterwhich we restore the azimuthal components to obtain the properties in the 4-dimensional setting.

3.1 The reduced unperturbed system

Consider the reduced unperturbed system:

$$\begin{aligned}
\dot{r}_1 &= r_1(\mu_1 + r_1^2 + br_2^2) \\
\dot{r}_2 &= r_2(\mu_2 + cr_1^2 + dr_2^2).
\end{aligned} \tag{6}$$

We first explore the central singularity at $(\mu_1, \mu_2) = (0, 0)$, and then its unfolding ($(\mu_1, \mu_2) \neq (0, 0)$).

3.1.1 The central singularity

Consider (6) for $\mu_1 = \mu_2 = 0$:

$$\begin{aligned}
\dot{r}_1 &= r_1(r_1^2 + br_2^2) \\
\dot{r}_2 &= r_2(cr_1^2 + dr_2^2).
\end{aligned} \tag{7}$$

[1] In this paper we consider $r_1 \geq 0$ and $r_2 \geq 0$.

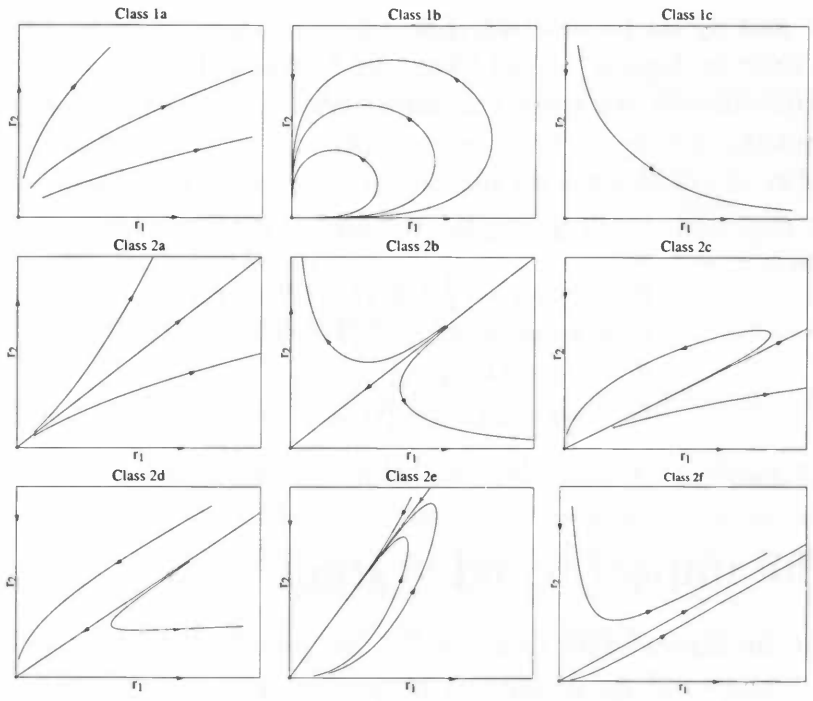

Figure 1: Phase portraits of the nine topological equivalence classes of (7).

Provided that $d - bc \neq 0$, this system has only one equilibrium, namely, $(r_1, r_2) = (0, 0)$.

For this case, there are nine topologically distinct equivalence classes [11, 17]. For a definition of topological equivalence, we refer to Arnold [1] or Palis & De Melo [16]. In this paper we follow the classification of [11], thus we do not distinguish between phase portraits that are equivalent up to reversal of time, and we do not allow interchanging of r_1 and r_2.

The phase portraits for these classes are given in Figure 1. Table 1 lists the conditions for each of the classes, and Figure 2 represents them in the (b, c)-plane.

The classes can be grouped into two types. The first type contains two invariant lines and the other three invariant lines. The zeros of the inner product

$$g = \left\langle \begin{bmatrix} r_1(r_1^2 + br_2^2) \\ r_2(cr_1^2 + dr_2^2) \end{bmatrix}, \begin{bmatrix} -r_2 \\ r_1 \end{bmatrix} \right\rangle = r_1 r_2 \{(c-1)r_1^2 + (d-b)r_2^2\} \qquad (8)$$

represent these lines. Hence the r_1 and r_2-axis are invariant lines, and the invariant line $r_2 = \sqrt{(1-c)/(d-b)}r_1$ exists only when $(1-c)/(d-b) > 0$ and $d - b \neq 0$.

Type 1 (two invariant lines)
$R1a = \{(b,c) : d = +1, bc \neq 1, \frac{1-c}{1-b} < 0\}$
$R1b = \{(b,c) : d = -1, bc \neq -1, \frac{1-c}{1-b} > 0, b < -1, c > 1\}$
$R1c = \{(b,c) : d = -1, bc \neq -1, \frac{1-c}{1-b} > 0, b > -1, c < 1\}$

Type 2 (three invariant lines)
$R2a = \{(b,c) : d = +1, \frac{1-c}{1-b} > 0, \frac{1-bc}{1-b} > 0\}$
$R2b = \{(b,c) : d = +1, \frac{1-c}{1-b} > 0, \frac{1-bc}{1-b} < 0\}$
$R2c = \{(b,c) : d = -1, \frac{1-c}{1+b} < 0, \frac{1+bc}{1+b} > 0, b < -1, c < 1\}$
$R2d = \{(b,c) : d = -1, \frac{1-c}{1+b} < 0, \frac{1+bc}{1+b} < 0, b < -1, c < 1\}$
$R2e = \{(b,c) : d = -1, \frac{1-c}{1+b} < 0, \frac{1+bc}{1+b} < 0, b > -1, c > 1\}$
$R2f = \{(b,c) : d = -1, \frac{1-c}{1+b} < 0, \frac{1+bc}{1+b} > 0, b > -1, c > 1\}$

Table 1: Conditions for the nine topological equivalence classes of (7). Note that R1a represents condition for topologically equivalence Class 1a, etc.

The direction of a flow at a point (r_1, r_2) not in the invariant lines can be determined by calculating the inner product (8). Regarding system (7), the flow is *turning to the left* if $g > 0$. If $g < 0$, it is *turning to the right.*

To determine the direction of a flow at a point (r_1, r_2) in one of the invariant lines, we substitute the point into inner product

$$f = \left\langle \begin{bmatrix} r_1(r_1^2 + br_2^2) \\ r_2(cr_1^2 + dr_2^2) \end{bmatrix}, \begin{bmatrix} r_1 \\ r_2 \end{bmatrix} \right\rangle = (b+c)r_1^2 r_2^2 + r_1^4 + dr_2^4. \tag{9}$$

If $f < 0$, the flow at that point has same direction as the direction of vector position of the point. If $f > 0$, it has opposite direction.

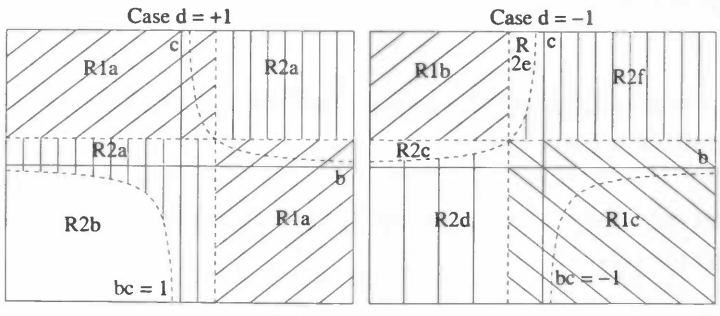

Figure 2: Diagram of conditions in the (b, c)-plane for the nine topological equivalence classes of (7).

3.1.2 Unfolding the central singularity

Now we analyse system (6) with $(\mu_1, \mu_2) \neq (0,0)$. For this case there can be up to four equilibria:

(i) $(r_1, r_2) = (0,0)$,

(ii) $(r_1, r_2) = (\sqrt{-\mu_1}, 0)$, for $\mu_1 < 0$,

(iii) $(r_1, r_2) = (0, \sqrt{-\frac{\mu_2}{d}})$, for $\mu_2 d < 0$,

(iv) $(r_1, r_2) = \left(\sqrt{\frac{b\mu_2 - d\mu_1}{d-bc}}, \sqrt{\frac{c\mu_1 - \mu_2}{d-bc}}\right)$, for $\frac{b\mu_2 - d\mu_1}{d-bc} > 0$ and $\frac{c\mu_1 - \mu_2}{d-bc} > 0$.

The classification as given in previous part is not the most natural when it comes to studying the unfoldings, because it considers the invariant line $r_2 = \sqrt{(1-c)/(d-b)}r_1$. Here there are twelve distinct cases, as set out in Table 2. Moreover, Figure 3 represents them in the (b,c)-plane. With this new classification, it is easier to study the unfoldings, since now only one open condition is considered, namely, $d - bc \neq 0$.

	RIa	RIb	RII	RIII	RIVa	RIVb
d	+1	+1	+1	+1	+1	+1
sign(b)	+	+	+	-	-	-
sign(c)	+	+	-	+	-	-
sign$(d-bc)$	+	-	+	+	+	-

	RV	RVIa	RVIb	RVIIa	RVIIb	RVIII
d	-1	-1	-1	-1	-1	-1
sign(b)	+	+	+	-	-	-
sign(c)	+	-	-	+	+	-
sign$(d-bc)$	-	+	-	+	-	-

Table 2: Sign-conditions for the twelve unfoldings of (7), where column RIa represents condition for Case Ia, etc.

Next we study the stability of the four equilibria. The linearized system of (6) has the matrix

$$\begin{bmatrix} \mu_1 + 3r_1^2 + br_2^2 & 2br_1r_2 \\ 2cr_1r_2 & \mu_2 + cr_1^2 + 3dr_2^2 \end{bmatrix}. \tag{10}$$

Analyzing the eigenvalues of this matrix, the following results hold.

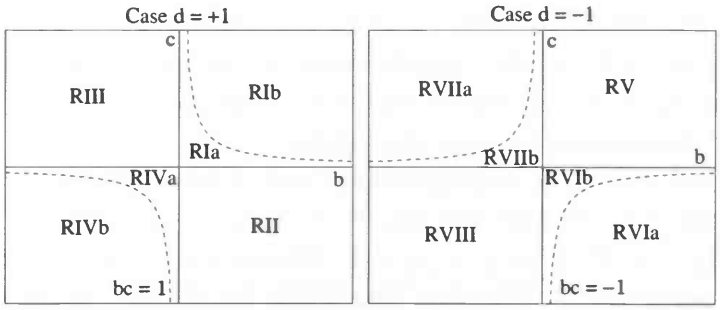

Figure 3: Diagram of the sign-conditions in the (b, c)-plane for the twelve unfoldings of (7).

(i) The equilibrium $(r_1, r_2) = (0, 0)$ is

  (a) a sink if both μ_1 and μ_2 are less than zero,

  (b) a source if both μ_1 and μ_2 are bigger than zero,

  (c) a saddle if μ_1 and μ_2 have different signs.

(ii) The equilibrium $(r_1, r_2) = (\sqrt{-\mu_1}, 0)$ is

  (a) a source if $\mu_2 - c\mu_1 > 0$,

  (b) a saddle if $\mu_2 - c\mu_1 < 0$.

(iii) The equilibrium $(r_1, r_2) = (0, \sqrt{-\mu_2/d})$ is

  (a) a sink if $d = -1$ and $\mu_1 + b\mu_2 < 0$,

  (b) a source if $d = 1$ and $\mu_1 - b\mu_2 > 0$,

  (c) a saddle if both $d = -1$ and $\mu_1 + b\mu_2 > 0$ hold or both $d = 1$ and $\mu_1 - b\mu_2 < 0$ hold.

(iv) The equilibrium $(r_1, r_2) = \left(\sqrt{\frac{b\mu_2 - d\mu_1}{d-bc}}, \sqrt{\frac{c\mu_1 - \mu_2}{d-bc}}\right)$ is

  (a) a sink if $d - bc > 0$, $d = -1$, and $b\mu_2 - d\mu_1 < d\mu_2 - cd\mu_1$,

  (b) a center if $d - bc > 0$, $d = -1$, and $b\mu_2 - d\mu_1 = d\mu_2 - cd\mu_1$,

  (c) a source if $d - bc > 0$ and $b\mu_2 - d\mu_1 > d\mu_2 - cd\mu_1$,

  (d) a saddle if $d - bc < 0$.

Crossing the line $\mu_1 = 0$ for $\mu_2 \neq 0$, pitchfork bifurcations occur at the point $(r_1, r_2) = (0, 0)$ in the one-dimensional center manifold given by the invariant line $r_2 = 0$. A center manifold is an invariant manifold tanget to the center eigenspace, i.e., the eigenspace corresponding to nonhyperbolic eigenvalues. For a detailed explanation of center manifold, we refer to Hirsch, Pugh, & Shub [13]. In this setting, $\dot{r}_1 = r_1(\mu_1 + r_1^2)$ and $\dot{r}_2 = 0$. A new equilibrium $(\sqrt{-\mu_1}, 0)$ is born at $\mu_1 = 0$. Meanwhile, crossing the line $\mu_2 = 0$ for $\mu_1 \neq 0$, pitchfork bifurcations also occur in the one-dimensional center manifold $r_1 = 0$. In this setting, $\dot{r}_1 = 0$ and $\dot{r}_2 = r_2(\mu_2 + dr_2^2)$. The new equilibrium is $(0, \sqrt{-\mu_2/d})$.

Apart from the point $(r_1, r_2) = (0, 0)$, pitchfork bifurcations occur at $(\sqrt{-\mu_1}, 0)$ when crossing the line $\mu_2 = c\mu_1$. They also occur at $(0, \sqrt{-\mu_2/d})$ when crossing the line $\mu_2 = \frac{d\mu_1}{b}$. The new equilibrium is $\left(\sqrt{\frac{b\mu_2 - d\mu_1}{d-bc}}, \sqrt{\frac{c\mu_1 - \mu_2}{d-bc}}\right)$.

Apart from the pitchfork bifurcations, there are also Hopf bifurcations. These bifurcations occur at the equilibrium $\left(\sqrt{\frac{b\mu_2 - d\mu_1}{d-bc}}, \sqrt{\frac{c\mu_1 - \mu_2}{d-bc}}\right)$, for (μ_1, μ_2) on the line

$$\mu_2 = \frac{\mu_1 d(1-c)}{(b-d)}, \tag{11}$$

or in case $d - bc > 0$ and $d = -1$. Hence they cannot occur in cases Ib, IVb, V, VIb, VIIb, and VIII, where $d - bc < 0$. Also they cannot occur in cases Ia, II, III, and IVa where $d = 1$. So Hopf bifurcations can occur only in cases VIa and VIIa.

To see that Hopf bifurcations occur at this equilibrium, we substitute (11) into system (6), obtaining:

$$\begin{aligned} \dot{r}_1 &= r_1(\mu_1 + r_1^2 + br_2^2) \\ \dot{r}_2 &= r_2\left(\mu_1 \tfrac{c-1}{b+1} + cr_1^2 - r_2^2\right). \end{aligned} \tag{12}$$

This system is integrable, since its solutions lie along level curves of the smooth function:

$$F(r_1, r_2) = r_1^{\alpha} r_2^{\beta}(\mu_1 + (r_1^2 + \gamma r_2^2)), \tag{13}$$

where $\alpha = 2(c-1)/(1+bc)$, $\beta = -2(1+b)/(1+bc)$, and $\gamma = (1+b)/(1-c)$. The level curves of this function in Case VIa can be seen in Figure 4 below. The phase portraits of the unfolding in Case Ia can be seen in Figure 5. In this paper, we show the unfoldings only for Case Ia and Case VIa, since the other cases can be obtained in similar way.

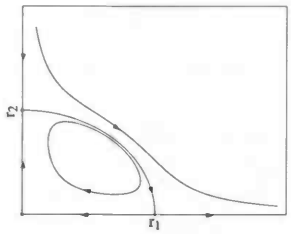

Figure 4: Level curves for Case VIa

3.2 Reconstruction

Now we restore the azimuthal components θ_1 and θ_2 and so reconstruct the results in the four dimensional setting. Recall that $\dot{\theta}_1 = \omega_1$ and $\dot{\theta}_2 = \omega_2$, then the following results hold.

(i) The equilibrium $(r_1, r_2) = (0, 0)$ corresponds to the equilibrium $(x, y, z, v) = (0, 0, 0, 0)$, since in this case $x = y = z = v = 0$ for every θ_1 and θ_2.

(ii) The equilibrium $(\sqrt{-\mu_1}, 0)$ corresponds to the periodic orbit

$$\{(\sqrt{-\mu_1}\cos(\omega_1 t), \sqrt{-\mu_1}\sin(\omega_1 t), 0, 0) : t \in \mathbb{R} \text{ is the time variable}\}.$$

(iii) The equilibrium $(0, \sqrt{-\mu_2/d})$ corresponds to the periodic orbit

$$\{(0, 0, \sqrt{-\mu_2/d}\cos(\omega_2 t), \sqrt{-\mu_2/d}\sin(\omega_2 t)) : t \in \mathbb{R}\}.$$

(iv) The invariant line $r_1 = 0$ corresponds to the invariant plane $\{(0, 0, z, v) : z, v \in \mathbb{R}\}$. This plane consists of spiral orbits. There is also a periodic orbit if the equilibrium $(0, \sqrt{-\mu_2/d})$ is on the line.

(v) The invariant line $r_2 = 0$ corresponds to the invariant plane $\{(x, y, 0, 0) : x, y \in \mathbb{R}\}$. This plane consists of spiral orbits. There is also a periodic orbit if the equilibrium $(\sqrt{-\mu_1}, 0)$ is on the line.

(vi) The equilibrium $\left(\sqrt{\frac{b\mu_2 - d\mu_1}{d-bc}}, \sqrt{\frac{c\mu_1 - \mu_2}{d-bc}}\right)$ corresponds to the invariant 2-torus

$$\left\{\left(\sqrt{\frac{b\mu_2 - d\mu_1}{d-bc}}\cos(\omega_1 t), \sqrt{\frac{b\mu_2 - d\mu_1}{d-bc}}\sin(\omega_1 t), 0, 0\right) : t \in \mathbb{R}\right\} \times$$
$$\left\{\left(0, 0, \sqrt{\frac{c\mu_1 - \mu_2}{d-bc}}\cos(\omega_2 t), \sqrt{\frac{c\mu_1 - \mu_2}{d-bc}}\sin(\omega_2 t)\right) : t \in \mathbb{R}\right\}.$$

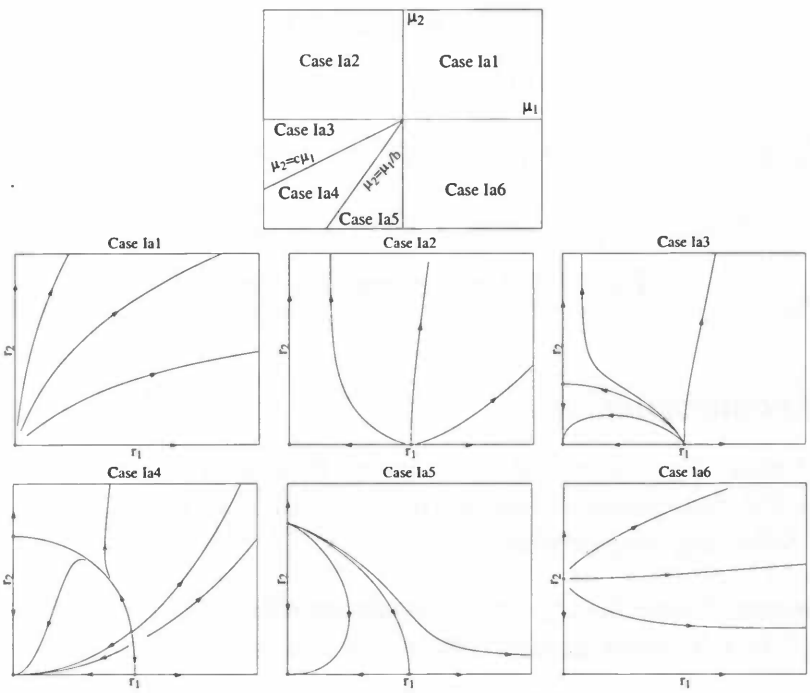

Figure 5: Unfolding for Case Ia.

(vii) The invariant line $r_2 = \sqrt{(1-c)/(d-b)}r_1$ corresponds to an invariant cone. This cone consists of spiral orbits.

(viii) Any periodic orbit $\gamma = \{(r_1(t), r_2(t)) : t \in \mathbb{R}\}$ in Case VIa or VIIa corresponds to the invariant 3-torus

$$\begin{aligned}&\{\{(p_1\cos(\omega_1 t), p_1\sin(\omega_1 t), 0, 0) : t \in \mathbb{R}\}\times\\ &\{(0, 0, p_2\cos(\omega_2 t), p_2\sin(\omega_2 t)) : t \in \mathbb{R}\}\times\\ &\{(p_1\cos(\omega_1 t), p_1\sin(\omega_1 t), p_2\cos(\omega_2 t), p_2\sin(\omega_2 t)) : t \in \mathbb{R}\} :\\ &(p_1, p_2) \in \gamma\}.\end{aligned}$$

This torus has quasi-periodic orbits with three independent frequencies. [2]

(ix) The Pitchfork bifurcations on the line $\mu_1 = 0$ and $\mu_2 = 0$ correspond to the two independent Hopf bifurcations in the 4-dimensional setting. Meanwhile, the Pitchfork bifurcations on the line $\mu_2 = c\mu_1$ and $\mu_2 = d\mu_1/b$ correspond to Neimark-Sacker bifurcations in the 4-dimensional setting. Crossing the line $\mu_2 = c\mu_1$ or $\mu_2 = d\mu_1/b$ results in the branching of a 2-dimensional torus from a periodic orbit [14].

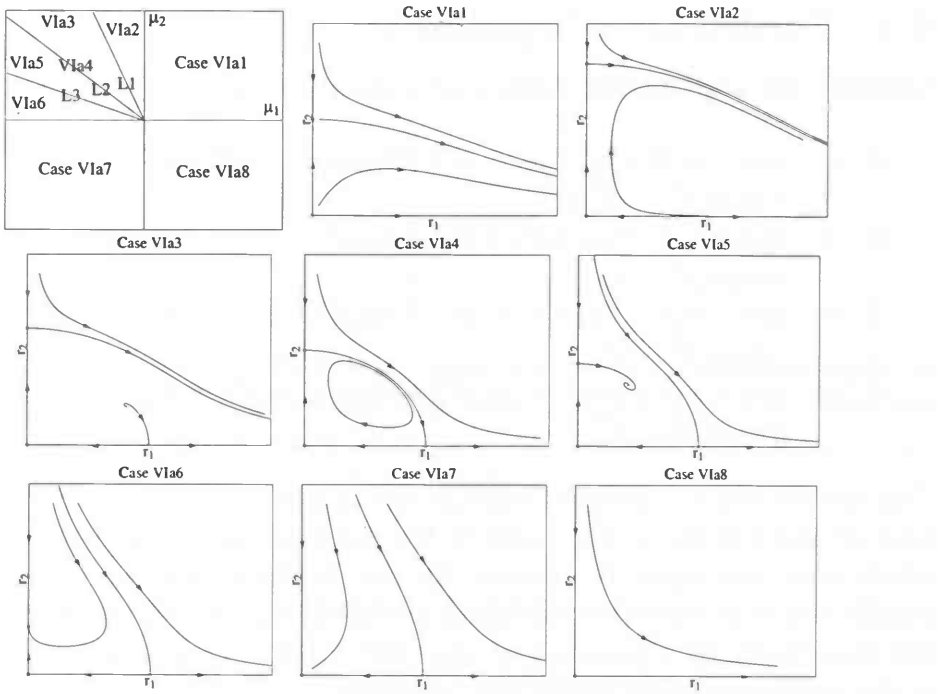

Figure 6: Partial unfolding for Case VIa. Note that the line L1 $\equiv \mu_2 = c\mu_1$, the line L2 $\equiv \mu_2 = \mu_1(c-1)/(b+1)$, and the line L3 $\equiv \mu_2 = -\mu_1/b$. The line L2 corresponds to Case VIa4.

4 The perturbed system

In this last section we consider the perturbed system (4), in other words, the original system (1) for small values of $\mathbf{x} = (x, y, z, v)$, μ_1 and μ_2. We investigate which dynamical properties can be derived from the dynamical properties of the unperturbed one.

4.1 Persistence of equilibria

Consider the unperturbed version of system (4), that is:

$$\begin{aligned}
\dot{x} &= \mu_1 x - \omega_1 y + a_{11}x(x^2+y^2) + a_{12}x(z^2+v^2) + a_{13}y(x^2+y^2) \\
&\quad -a_{14}y(z^2+v^2) \\
\dot{y} &= \mu_1 y + \omega_1 x + a_{11}y(x^2+y^2) + a_{12}y(z^2+v^2) - a_{13}x(x^2+y^2) \\
&\quad +a_{14}x(z^2+v^2) \\
\dot{z} &= \mu_2 z - \omega_2 v + a_{21}z(x^2+y^2) + a_{22}z(z^2+v^2) - a_{23}v(x^2+y^2) \\
&\quad -a_{24}v(z^2+v^2) \\
\dot{v} &= \mu_2 v + \omega_2 z + a_{21}v(x^2+y^2) + a_{22}v(z^2+v^2) + a_{23}z(x^2+y^2) \\
&\quad +a_{24}z(z^2+v^2).
\end{aligned} \tag{14}$$

This system has a hyperbolic equilibrium at point $\bar{\mathbf{x}} = (0,0,0,0)$. The linear part of this system at the point $\bar{\mathbf{x}}$ has determinant as $(\mu_1^2+\omega_1^2)(\mu_2^2+\omega_2^2)$ which does not equal 0. Hence, by the Implicit Function Theorem, the equilibrium is persistent under small perturbations. Moreover since the point $\bar{\mathbf{x}}$ is hyperbolic, by Theorem 2 on page 305 of [12], the hyperbolic equilibrium is also persistent under small perturbations.

4.2 On the periodic orbits

For certain values of μ_1 and μ_2, we know that system (14) has periodic orbits on the (x,y)-plane and the (z,v)-plane. We can't determine the persistence of these orbits, because the Implicit Function Theorem can't be applied directly, because the corresponding Poincaré map has an eigenvalue as 1.

4.3 Application of KAM Theory

Considering the higher order normalization (the fifth-order terms) in the 2-dimensional reduced system, there is an attracting limit cycle in Case VIa and Case VIIa [11, 14]. A careful analysis based on Pontryagin's technique and nontrivial estimates of Abelian integrals shows that our system can have no more than one limit cycle [14].

Figure 7 describes the location of the cycle and the cycle itself for Case VIa. This limit cycle corresponds to an invariant 3-torus in the 4-dimensional original system. The hyperbolicity of this limit cycle leads to the normal hyperbolicity of the torus. According to the center manifold theorem, Theorem 4.1 [13], it follows that this torus as an invariant manifold is persistent.

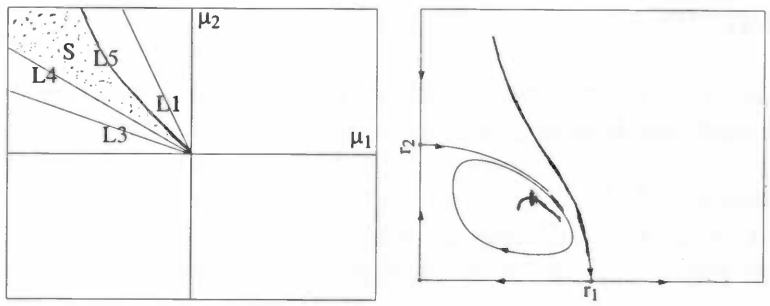

Figure 7: *Left picture*: dotted area S represents the location of limit cycle for Case VIa. *Right picture*: the attracting limit cycle for Case VIa. Note that the line L1 $\equiv \mu_2 = c\mu_1$, the line L3 $\equiv \mu_2 = -\mu_1/b$, the line L4 $\equiv \mu_2 = -\mu_1$, and the line L5 represents a quadratic function.

The parallel dynamics on this torus is determined by

$$\begin{aligned}
\dot{\theta}_1 &= \omega_1 + \text{l.o.t}(|\mu_1, \mu_2|) + \text{h.o.t}(|\mu_1, \mu_2|) \\
&= \Omega_1(\mu_1, \mu_2) + \text{h.o.t}(|\mu_1, \mu_2|) \\
\dot{\theta}_2 &= \omega_2 + \text{l.o.t}(|\mu_1, \mu_2|) + \text{h.o.t}(|\mu_1, \mu_2|) \\
&= \Omega_2(\mu_1, \mu_2) + \text{h.o.t}(|\mu_1, \mu_2|) \\
\dot{\theta}_3 &= \omega_3(\mu_1, \mu_2) + \text{l.o.t}(|\mu_1, \mu_2|) + \text{h.o.t}(|\mu_1, \mu_2|) \\
&= \Omega_3(\mu_1, \mu_2) + \text{h.o.t}(|\mu_1, \mu_2|),
\end{aligned} \tag{15}$$

where the l.o.t$(|\mu_1, \mu_2|)$-terms can be obtained by averaging method, and the function $\omega_3(\mu_1, \mu_2)$ by the elliptic integral (see [18, 15, 9] for a detailed description).

This parallel dynamics is persistent under small perturbations [6, 8] if the frequency vector $O = (\Omega_1, \Omega_2, \Omega_3)$ satisfies the Diophantine condition

$$| < k, O > | \geqslant \frac{\gamma}{|k|^\tau},$$

for all $k \in \mathbb{Z}^3 - \{0\}$, and $\gamma > 0$, $\tau > 2$ are given.

To pullback the solutions of Diophantine condition from the $(\Omega_1, \Omega_2, \Omega_3)$-space into the (μ_1, μ_2)-plane, we need to consider map $\Omega : \mathbb{R}^2 \to \mathbb{R}^3$ given by $(\mu_1, \mu_2) \mapsto (\Omega_1(\mu_1, \mu_2), \Omega_2(\mu_1, \mu_2), \Omega_3(\mu_1, \mu_2))$ that probably has maximal rank. Then we have the following conjecture.

Conjecture 2 *There is a Cantor (contains dust), inside the area S with quasi-periodic 3-tori. This Cantor set has measure bigger than zero, which tends to full measure near* $(\mu_1, \mu_2) = (0, 0)$.

References

[1] Arnold, V.I., *Geometrical Methods in the Theory of Ordinary Differential Equations*, Springer Verlag, 1983.

[2] Braaksma, B.L.J., Broer,H.W., Quasi periodic flow near a codimension one singularity of a divergence free vector field in dimension four, *Bifurcation, théorie ergodique et applications, Astérisque*, **98-99**, pp.74-142, 1982.

[3] Broer, H.W., van Strien, S.J., *Infinitely many moduli of strong stability in divergence free unfoldings of singularities of vector fields*, Lecture note in Mathematics **1007**, Springer Verlag, pp. 39-59, 1983.

[4] Broer, H.W., Vegter, G., Subordinate Sil'nikov bifurcations near some singularities of vector fields having low codimension, *Ergod. Th. & Dynam. Sys.*, **6**, pp. 509-525, 1984.

[5] Broer, H.W., Takens, F., Formally symmetric normal forms and genericity, *Dynamics Reported*, **2**, pp. 36-60, 1989.

[6] Broer, H.W., Huitema, G.B., Takens, F., Unfoldings of Quasi-Periodic Tori, *AMS.* **83**(421), pp. 1-82, 1990.

[7] Broer, H.W., *Notes on Perturbation Theory*, Lecture Notes Erasmus Course Diepenbeek, 1992.

[8] Broer, H.W., Huitema, G.B., Sevryuk, M.B., *Quasi-Periodic Motions in Families of Dynamical Systems*, Lecture note in Mathematics **1645**, Springer Verlag, 1996.

[9] Broer, H.W., Quasi-periodicity in dissipative systems, *MIHMI*, 2000.

[10] Chow, S-N., Li, C., Wang, D., *Normal Forms and Bifurcation of Planar Vector Fields*, Cambridge University Press, 1994.

[11] Guckenheimer, J., Holmes, P., *Nonlinear Oscillations, Dynamical Systems, and Bifurcations of Vector Fields*, Springer Verlag, 1983.

[12] Hirsch, M.W., Smale, S., *Differential Equations, Dynamical Systems, and Linear Algebra*, Academic Press, 1974.

[13] Hirsch, M.W., Pugh, C.C., Shub, M., *Invariant Manifolds*, LNM **583**, Springer Verlag, 1977.

[14] Kuznetsov, Y.A., *Elements of Applied Bifurcation Theory*, Springer Verlag, 1995.

[15] Scheurle, J., Marsden, J.E., Bifurcation to quasi-periodic tori in the interaction of steady state and Hopf bifurcations, *Siam J. Math. Anal.*, **15**, pp. 1055-1074, 1984.

[16] Palis, J. Jr., de Melo, W., *Geometric Theory of Dynamical System: An Introduction*, Springer Verlag, 1982.

[17] Takens, F., Singularities of Vector Fields, *Publ. Math. IHES*, **43**, pp. 47-100, 1974.

[18] Zoladek, H., Bifurcations of a certain family of planar vector fields tangent to axes, *Journ. Diff. Eqns*, **67**, pp. 1-55, 1987.